Article

pubs.acs.org/Biomac

Sequential Thiol–Ene and Tetrazine Click Reactions for the Polymerization and Functionalization of Hydrogel Microparticles

Faraz Jivan,[†,∥] Ramanathan Yegappan,[†,∥] Hannah Pearce,[†] James K. Carrow,[†] Michael McShane,[†,‡] Akhilesh K. Gaharwar,[†,‡,§] and Daniel L. Alge*[,†,‡]

[†]Department of Biomedical Engineering, [‡]Department of Materials Science and Engineering, and [§]Center for Remote Health Technologies and Systems, Texas A&M University, College Station, Texas 77843, United States

Supporting Information

ABSTRACT: Click chemistry is a versatile tool for the synthesis and functionalization of polymeric biomaterials. Here, we describe a versatile new strategy for producing bioactive, protein-functionalized poly(ethylene glycol) (PEG) hydrogel microparticles that is based on sequential thiol–ene and tetrazine click reactions. Briefly, tetra-functional PEG-norbornene macromer and dithiothreitol (SH) cross-linker were combined at a 0.75:1 [SH]:[norbornene] ratio, emulsified in a continuous Dextran phase, and then photopolymerized to form PEG hydrogel microparticles that varied from 8 to 30 μm in diameter, depending on the PEG concentration used. Subsequently, tetrazine-functionalized protein was conjugated to unreacted norbornene groups in the PEG microparticles. Tetrazine-mediated protein tethering to the microparticles was first demonstrated using fluorescein-labeled ovalbumin as a model protein. Subsequently, bioactive protein tethering was demonstrated using alkaline phosphatase (ALP) and glucose oxidase (GOx). Enzyme activity assays demonstrated that both ALP and GOx maintained their bioactivity and imparted tunable bioactivity to the microparticles that depended on the amount of enzyme added. ALP-functionalized microparticles were also observed to initiate calcium phosphate mineralization *in vitro* when incubated with calcium glycerophosphate. Collectively, these results show that protein-functionalized hydrogel microparticles with tunable bioactive properties can be easily synthesized using sequential click chemistry reactions. This approach has potential for future applications in tissue engineering, drug delivery, and biosensing.

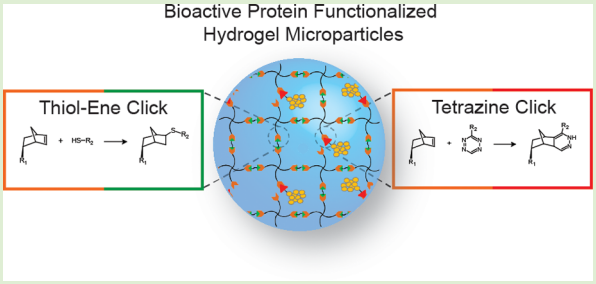

1. INTRODUCTION

Click chemistry is a versatile tool for the synthesis and functionalization of polymeric biomaterials. Click chemistry encompasses a chemical toolkit of highly efficient, specific, and high-yielding reactions that can be performed under mild conditions and produce inoffensive byproducts.[1] Two notable click reactions that are gaining importance for biological applications are the thiol–ene and bioorthogonal tetrazine reactions. The thiol–ene click reaction, which refers to the radical-mediated addition of a thiol to a nonsterically hindered alkene (e.g., norbornene), is being used extensively in polymer synthesis.[2−5] Key advantages of thiol–ene click reactions include their insensitivity to oxygen and the potential for rapid yet stoichiometrically controlled polymerization, which can be further kinetically controlled via photoinitiation.[6,7] Thiol–ene click chemistry has also been used to achieve facile incorporation of synthetic peptides and proteins into hydrogel biomaterials, which has led to its broad adoption in the preparation of extracellular matrix mimics for tissue engineering.[8−13] Bio-orthogonal tetrazine click reactions are a different class of addition reactions that proceed spontaneously via an inverse electron-demand Diels–Alder cycloaddition between tetrazines and electron-rich alkenes, such as norbornene and trans-cyclooctene.[14] Importantly, tetrazine click reactions can proceed with fast reaction rates, do not require radical initiation, can be performed in aqueous conditions at physiologic temperature and pH, and are generally compatible with cells and biologics.[15,16] Thus, tetrazine click chemistry is considered to be bioorthogonal. Bioorthogonal tetrazine ligation has been used for both *in vitro* and *in vivo* cell labeling,[17−20] polymer coupling,[16] and cell encapsulation within bioactive hydrogels.[21,22] Tetrazine click chemistry is also synthetically tractable for biomaterials scientists, as gram-scale quantities of asymmetric tetrazines suitable for bioconjugation and polymer functionalization can be readily synthesized.[23] This is an important advantage compared to other bioorthogonal click reactions.

We are interested in applying click chemistry to the development of hydrogel microparticles due to their utilization in a variety of medical and biological applications spanning from drug delivery to tissue engineering and regenerative medicine.[24−27] Griffin et al. recently reported using hydrogel microparticles as injectable building blocks for macroporous scaffolds, which they showed accelerated wound healing *in*

Received: July 2, 2016
Revised: September 21, 2016
Published: September 22, 2016

DOI: 10.1021/acs.biomac.6b00990
Biomacromolecules 2016, 17, 3516−3523

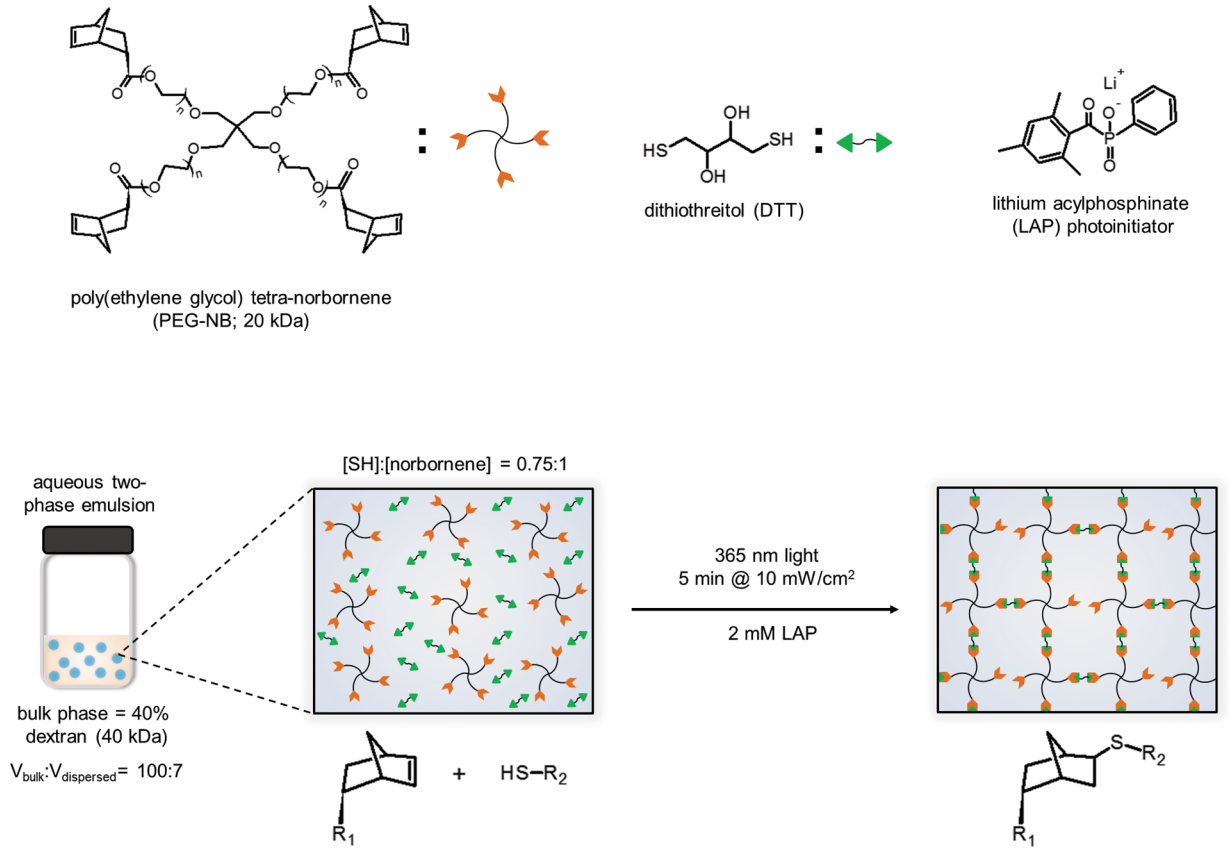

Figure 1. Chemical structures and schematic of PEG microparticle synthesis using thiol−ene click chemistry. Top Panel: Chemical structures for monomers poly(ethylene glycol) tetra-norbornene (PEG-NB), represented by 4 arm stars, and dithiothreitol (DTT), represented by linear chains, along with photoinitiator lithium acylphosphinate (LAP) are shown. Bottom Panel: A dispersed phase consisting of PEG-NB, DTT (0.75:1 thiol−ene ratio), and LAP were emulsified in a bulk phase consisting of 40 kDa dextran and LAP (100 bulk:7 disperse, by vol.). The emulsion was photopolymerized at 365 nm light for 5 min at 10 mW/cm^2 to yield hydrogel microparticles with 25% unreacted norbornene groups. The figure depicts an idealized hydrogel network.

vivo.[28] This exciting work highlights an emerging application for hydrogel microparticles in the production of three-dimensional (3D) scaffolds with enhanced regenerative capabilities, as opposed to their common use as discrete microdevices for drug and cell delivery. Hydrogel microparticles are routinely synthesized by liquid−liquid phase separation using solution, suspension, or emulsion polymerization-based strategies.[29,30] The general approach of liquid−liquid two phase polymerization is useful because it is simple to perform and can be easily scaled up to quickly produce large batches of microparticles, for example, when photopolymerization is employed. Recently, Parlato et al. demonstrated the fabrication of hydrolytically- and enzymatically degradable poly(ethylene glycol) (PEG) microparticles that were tens of microns in diameter by vinyl photopolymerization within a water-in-water emulsion.[26] Young et al. employed vinyl photopolymerization in combination with submerged electrospraying in oil to produce larger microparticles (hundreds of microns in diameter) under conditions that were suitable for cell encapsulation.[31]

It should be appreciated that the implementation of click chemistry can advance the production of bioactive hydrogel microparticles and lead to new applications in drug delivery and tissue engineering. Indeed, click-based approaches have been used to synthesize hydrogel microparticles incorporating bioactive agents. For example, the previously cited study by Griffin et al. used the thiol-vinyl sulfone Michael addition, which is a base-catalyzed click reaction, to make hydrogel microparticles containing peptide sequences that were critical to their microparticle annealing approach.[28] In another recent study, Belair et al. used photoinitiated thiol−ene click chemistry to produce peptide-functionalized hydrogel microparticles capable of sequestering and releasing vascular endothelial growth factor.[32] This approach is particularly interesting, as the fast kinetics and efficiency of photoinitiated thiol−ene click chemistry make it well suited for batch microparticle synthesis. Moreover, the use of norbornene as the alkene provides a unique opportunity to combine thiol−ene and tetrazine click reactions for hydrogel microparticle synthesis and functionalization in a potentially synergistic way by capitalizing on norbornene's reactivity with tetrazines.[16,17,20−22,33−37] In our opinion, bioorthogonal tetrazine click chemistry is particularly well-suited for functionalizing prefabricated batches of microparticles with bioactive proteins, as this strategy completely avoids exposing the protein to potentially damaging conditions during microparticle fabrication, which could be critical when working with fragile proteins.

Therefore, the objective of this study was to combine thiol−ene and tetrazine click chemistry in a sequential process to develop a versatile and tunable platform for producing protein-functionalized bioactive hydrogel microparticles. The proposed approach combines the benefits of thiol−ene click chemistry (rapid microparticle synthesis, stoichiometric control, tunable material properties, and potential for scale-up) with tetrazine

DOI: 10.1021/acs.biomac.6b00990
Biomacromolecules 2016, 17, 3516−3523

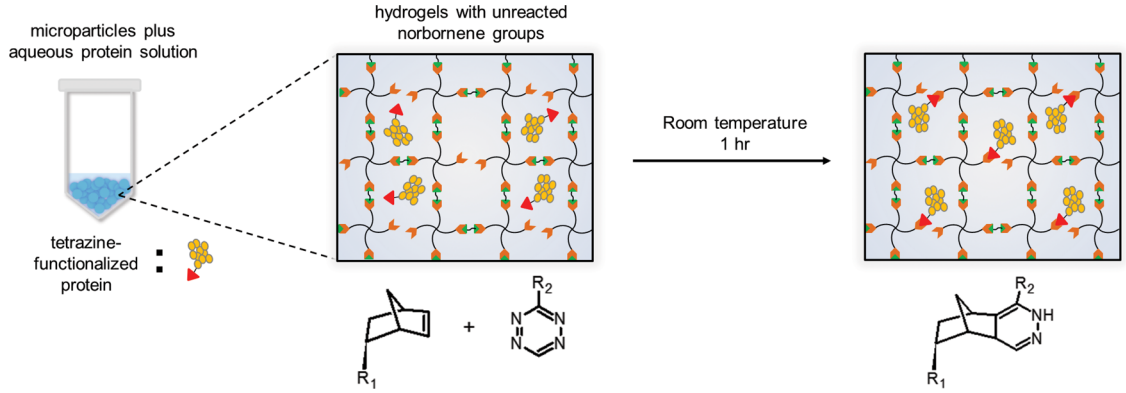

Figure 2. Chemical structures and schematic of protein-functionalized microparticles using tetrazine-norbornene click chemistry. Pelleted microparticles were incubated for 1 h at room temperature with tetrazine-functionalized protein to allow them to "click" onto the previously unreacted norbornene groups present in the microparticles and yield bioactive, protein-functionalized hydrogel microparticles. The figure depicts an idealized hydrogel network.

click chemistry to achieve click-mediated protein incorporation into microparticles while preserving native function. To this end, thiol-norbornene and tetrazine-norbornene click reactions were used sequentially to fabricate hydrogel microparticles by performing the thiol−ene polymerization off-stoichiometry (0.75:1.0 thiol-to-norbornene ratio) and then chemically conjugating tetrazine-functionalized proteins to the remaining norbornene groups. PEG concentration was varied to characterize its effect on microparticle size. Efficacy of the tetrazine bioconjugation reaction was then tested using fluorescein-labeled ovalbumin as a model protein. Finally, alkaline phosphatase (ALP) and glucose-oxidase (GOx) were tested to demonstrate utility with bioactive proteins and quantitatively assess microparticle bioactivity.

2. EXPERIMENTAL SECTION

2.1. PEG-Tetra Norbornene (PEG-NB) Synthesis. A PEG-NB precursor for hydrogel microparticles was synthesized according to a previously described method with slight variation.[8] Briefly, 5.0 g PEG macromer (20 kDa, 4-arm PEG-hydroxyl, JenKem), 4-(dimethylamino)pyridine (0.5X to PEG-OH, Sigma-Aldrich), pyridine (5X to PEG-OH, Sigma-Aldrich), and anhydrous dichloromethane (20 mL) were dissolved in round-bottom flask under argon. Separately, 5-Norbornene-2-carboxcylic acid (10 COOH:1 PEG-OH, Alfa Aesar; predominantly endo isomer), diisopropylcarbodiimde (Alfa Aesar) anhydrous dichloromethane (15 mL, Acros) were mixed for 30 min at room temperature in a reaction vessel under argon to generate a dinorbornene anhydride, which was filtered to remove precipitated urea salts and then added to the round-bottom flask containing PEG. The solution was allowed to react overnight at room temperature, after which it was precipitated in 10-fold vol. excess of diethyl ether (Thermo Fisher) and vacuum filtered to yield a white precipitate (PEG-NB). The PEG-NB was subsequently dried under vacuum for 24 h, dialyzed against deionized water for 2 days (MWCO = 10 kDa), and lyophilized to obtain quantitative yield of purified PEG-NB. Analysis by ^{1}H NMR indicated quantitative end-group functionalization with norbornene (Supporting Information, Figure S1).

2.2. PEG Thiol−Ene Microparticle Synthesis and Characterization. Microparticles were synthesized via an aqueous two-phase emulsion system based on bulk phase dextran-disperse phase PEG polymer immiscibility[32] (Figure 1). Briefly, a dispersed phase consisting of varying wt % PEG-NB macromer (7.5 wt %, 10 wt %, 15 wt %), dithiothreitol (0.75:1.0 thiol−ene, Alfa Aesar) and lithium phenyl-2,4,6-trimethylbenzoylphosphinate photoinitiator (LAP, 2 mM; synthesized as previously described;[38] Supporting Information, Figure S2), was emulsified in a bulk phase of dextran (40 wt %, 40 kDa, BioChemica) and LAP (3.125 mM). Emulsions were vortexed and allowed to sit for 10 min to allow for phase separation and then photopolymerized with 365 nm UV light (10 mW/cm^2, 5 min, Lumen Dynamics Omnicure S2000 Series). The resulting microparticles were pelleted via centrifugation (4400 rpm, 10 min) in PBS (30:1 by vol.). The supernatant was decanted and the microparticles were viewed using bright field microscopy (10X, Nikon Eclipse TE2000-S). Microparticle diameters were determined from bright field images analyzed using the ImageJ Particle Analyzer tool (NIH), and a size distribution histogram was plotted for the varying PEG concentrations). Microparticles were stored long-term in PBS and were stable against hydrolysis at neutral pH, as expected.[39] Microparticles prepared with 10 wt % PEG-NB were used for subsequent protein conjugation experiments.

2.3. Characterization of Norbornene Conversion via Sequential Thiol−ene and Tetrazine Click Reactions. 5-(4-(1,2,4,5-Tetrazin-3-yl)benzylamino)-5-oxopentanoic acid was synthesized by reacting 5-(4-(cyano)benzylamino)-5-oxopentanoic acid with hydrazine, formamidine acetate, and zinc triflate catalyst, as previously described.[17] This tetrazine was subsequently converted to a succinimidyl ester upon reaction with *N,N′*-disuccinimidyl carbonate and triethylamine in acetonitrile according to the method of Han et al.[20] The resulting tetrazine NHS ester (Tz-NHS, Supporting Information, Figure S3) was purified by flash chromatography and verified by electrospray ionization mass spectrometry ([M + H] predicted = 399.1, actual = 399.1). To characterize norbornene conversion via sequential thiol−ene and tetrazine click reactions, hydrogels were cross-linked with dithiothreitol and functionalized to varying extents with Tz-NHS. Samples were prepared at 0.75:1 [SH]:[ene] ratio, 0.75:1 [SH]:[ene] ratio followed by 0.25:1 [Tz]:[ene], and 0.75:1 [SH]:[ene] ratio followed by 0.4:1 [Tz]:[ene] (i.e., excess tetrazine). Samples were degraded in 0.01 M sodium hydroxide overnight to hydrolyze ester linkages between norbornene and PEG, pH equilibrated with equimolar hydrochloric acid, then frozen at −80 °C and lyophilized for 2 days. Lyophilized product was

DOI: 10.1021/acs.biomac.6b00990
Biomacromolecules 2016, 17, 3516−3523

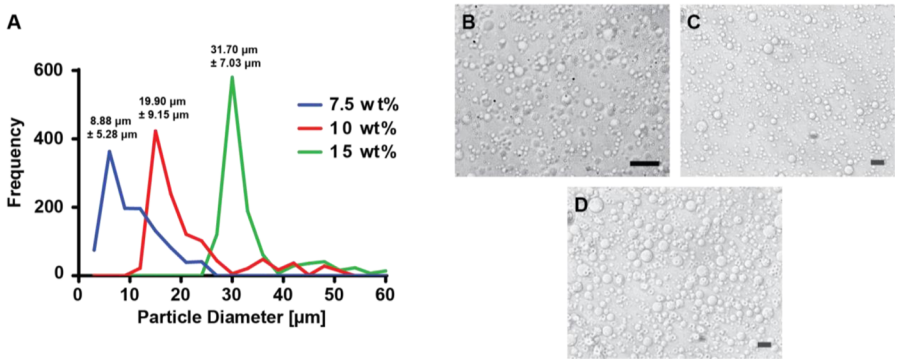

Figure 3. Particle size variation with PEG-NB concentration. (A) Histogram of particle size for microparticles synthesized with each PEG concentration (7.5, 10, 15 wt %) is plotted, along with the calculated average particle size and standard deviation (n = 1124) noted above each peak. Data was analyzed by one-way ANOVA followed by post hoc comparisons (Tukey's method). Statistical analysis showed average particle size significantly increased with PEG concentration ($p < 0.05$). (B–D) Bright-field, grayscale images of microparticles for the increasing PEG concentrations are shown. Scale bars = 50 μm.

dissolved in a mixture of deuterated solvents (50:50, deuterium oxide: dimethyl sulfoxide-d6) and ^{1}H NMR was performed on a 300 MHz instrument to quantify conversion of alkene protons on norbornene.

2.4. Protein-Functionalization with Tetrazine Click Chemistry. *2.4.1. General Approach.* For protein functionalization, 100 mM Tz-NHS dissolved in DMSO, was added to the protein of interest (10-fold molar excess tetrazine to protein) in PBS, and allowed to incubate at room temperature for 1 h to allow for tetrazine conjugation to amines of the protein (Tz-Protein). Subsequent protein functionalization of the microparticles was achieved by incubating pelleted microparticles with Tz-Protein at room temperature for 1 h (Figure 2). Microparticles were then washed three times with PBS (10,000 rpm, 5 min) to remove unconjugated Tz-Protein. The microparticle pellet was resuspended in PBS (600 μL), and further testing was performed based on the conjugated protein of interest.

2.4.2. Fluorescein–Ovalbumin. Fluorescein–ovalbumin (5 mg/mL, Life Technologies) in PBS was tetrazine functionalized (Tz-Ovalbumin) and conjugated to the microparticles as described above. Incubation with the microparticle pellet was also performed using fluorescein–ovalbumin without tetrazine functionalization (NF-Ovalbumin), which served as a negative control for protein tethering with the tetrazine–norbornene click reaction. After the microparticle pellet was resuspended in PBS, the microparticles were imaged using fluorescence microscopy (Nikon Eclipse TE2000-S). Their fluorescence was quantified by analysis on a flow cytometer (BD Accuri C6).

2.4.3. Alkaline Phosphatase. Alkaline phosphatase (ALP) from bovine intestinal mucosa (Sigma-Aldrich) was dissolved in PBS (50 mg/mL). Tetrazine functionalization (Tz-ALP) and microparticle conjugation were performed as described above. A negative control for microparticle conjugation was also prepared with nonfunctionalized ALP (NF-ALP). Prior to microparticle conjugation, Tz-ALP and NF-ALP were compared to ensure tetrazine conjugation did not affect bioactivity (Supporting Information, Figure S4).

To study dose-dependent ALP bioactivity, microparticles were loaded with varying amounts of NF-ALP and Tz-ALP (ranging from 0 mg/mL – 25 mg/mL). Microparticles were added to para-nitrophenylphosphate substrate (pNPP, Sigma-Aldrich) in a 96-well plate, and the change in absorbance at 405 nm was monitored over time on a microplate reader (TECAN Infinite M200 Pro). The absorbance increases over time were plotted, and the slopes of the data sets were compared to determine ALP activity.

To demonstrate ALP-induced mineralization, 0.1 M calcium glycerophosphate (Alfa Aesar) dissolved in milli-Q water was incubated with Tz-ALP conjugated microparticles and control NF-ALP microparticles at 37 °C for 1 h. A negative control of calcium glycerophosphate without microparticles was also tested. Microparticles and any precipitated solids were then centrifuged and washed three times with milli-Q water (10 000 rpm, 5 min) prior to mineralization staining. Alizarin red S (2%, pH 4.2, Electron Microscopy Sciences) was filtered through 25 mm syringe-tip, nylon membrane filter (0.45 μm) and incubated with the microparticles at room temperature for 10 min. The microparticles were subsequently washed three times with milli-Q water and visualized in bright field for red-stained calcium deposits on an inverted microscope (Nikon Eclipse TE2000S). To quantify alizarin red S staining, the microparticles were destained by incubating with 10% glacial acetic acid at room temperature for 30 min, after which the microparticles were pelleted by centrifugation (10 000 rpm, 5 min) and the supernatant was collected. Ten percent ammonium hydroxide was added to the supernatant to return the red color and acidic pH (4.1–4.5). The absorbance at 405 nm was then quantified on a microplate reader.

2.4.4. Glucose Oxidase. Glucose oxidase (GOx) was dissolved in PBS (50 mg/mL), functionalized with tetrazine (Tz-GOx), and then conjugated to microparticles, as described above. A negative control for microparticle conjugation was also prepared with nonfunctionalized GOx (NF-GOx). Prior to microparticle conjugation, Tz-GOx and NF-GOx were compared to ensure tetrazine conjugation did not affect bioactivity (Supporting Information, Figure S5).

To study dose-dependent GOx enzyme bioactivity, microparticles were loaded with varying amounts of NF-GOx and Tz-GOx (ranging from 0 mg/mL to 8 mg/mL). Microparticles were washed three times in PBS to remove unconjugated protein, and equilibrated in sodium acetate buffer (pH 5) for 1 h. An adaptation of an established protocol[40] was used to quantify GOx bioactivity. Briefly, NF-GOx- and Tz-GOx-conjugated microparticles were incubated in a solution of D-glucose (1.67 wt %), horseradish peroxidase (0.007 mg/mL), and o-dianisidine dye (1.68 μM) in sodium acetate buffer in a 96-well plate, and the change in absorbance at 490 nm was

DOI: 10.1021/acs.biomac.6b00990
Biomacromolecules 2016, 17, 3516–3523

monitored over time on a microplate reader. The absorbance increases over time were plotted, and the slopes of the data sets were compared to determine GOx activity.

2.5. Statistical Analysis. Particle size data was statistically analyzed in GraphPad Prism 6 using one-way ANOVA followed by post hoc comparisons between PEG weight percentages using Tukey's method. More than 1000 particle diameters were measured from bright field images using ImageJ. Additionally, both ALP and GOx data were statistically using two-way ANOVA with loaded protein concentration and functionalization (i.e., tetrazine-functionalized vs nonfunctionalized) as the main effects. Post hoc comparisons between groups were performed using Tukey's method. ALP and GOx data sets were analyzed using results from three independent trials. In all cases, statistically significant data was determined with a p-value of <0.05.

3. RESULTS AND DISCUSSION

3.1. Thiol−ene Polymerization of Hydrogel Microparticles. Key advantages to using photoinitiated thiol−ene click chemistry in conjunction with the emulsion-based microparticle synthesis are the rapid gelation times, stoichiometric control, tunability of material properties, and potential for scale up. We first characterized microparticle size using the thiol−ene polymerization and polymer immiscibility emulsion. Microparticles were synthesized with different concentrations of PEG-NB macromer (7.5, 10, and 15 wt %), and bright field images were analyzed in Image-J to determine average particle size of these different batches. In order to select a maximum number of particles in each image without background interference, a low threshold was set prior to obtaining particle diameters. More than 1000 particles were analyzed for each PEG-NB wt % variation. The data showed that as PEG-NB wt % increased, average particle size also significantly increased (p < 0.05) from 8.88 μm ± 5.28 to 31.7 μm ± 7.03 μm (Figure 3). The increase in particle size could be attributed directly to an increase in PEG content, which increases the volume of polymer as well as the total volume of water in the microparticles at equilibrium swelling. The 15 wt % group also appeared to have lower polydispersity, which could potentially be attributed to a reduction in the occurrence of network nonidealities at higher polymer concentrations.[36,39,41]

Hydrogel microparticle size is just one of several important variables that could affect the performance of these materials for applications in tissue engineering and drug delivery. In addition, other variables besides PEG concentration that were not investigated here but could be tuned to modulate the properties of the microparticles include the PEG molecular weight, the PEG-arm functionality, and the length of the dithiol cross-linker. The addition of enzymatically degradable linkers (i.e., matrix metalloproteinase degradable peptides) in particular could enhance the utility of these microparticles, for example by facilitating the enzymatically triggered release of a therapeutic growth factor for regenerative medicine.[42−45] Future work will focus on this possibility, as well as increasing average particle size to hundreds of microns in diameter for applications in cell delivery. Additionally, although the polydispersity of the microparticles did not affect other aspects of this project, we will explore methods such as dropwise polymerization from a water-in-oil emulsion (e.g., submerged electrospraying,[31] microfluidics[28]) to generate more monodisperse batches without compromising fabrication scalability.

3.2. Norbornene Conversion via Sequential Click Reactions. To demonstrate the stoichiometric control of the thiol−ene click and that the unreacted norbornenes can subsequently participate in tetrazine click reactions, norbornene conversion was quantified by ^{1}H NMR and compared to unreacted PEG-NB (Figure 4). Conversion of norbornene

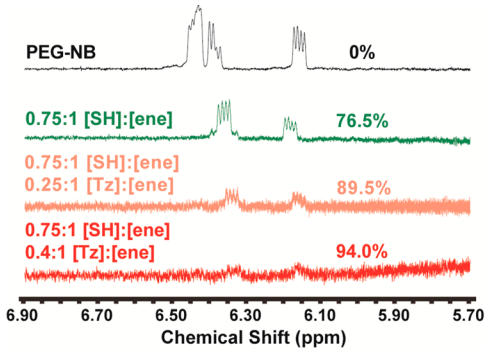

Figure 4. ^{1}H NMR characterization of norbornene conversion. The peaks corresponding to the alkene protons of norbornene were markedly reduced after cross-linking at a 0.75:1 [SH]:[ene] ratio, and integration relative to the ethylene glycol protons of PEG revealed 76.5% conversion in the thiol−ene click reaction. Subsequent reductions corresponding to 89.5% and 94% conversion were observed when tetrazine was added, indicating that the residual norbornene groups were accessible for tetrazine click functionalization.

groups inversely correlated with the integration of alkene hydrogen peaks. As expected, norbornene conversion was approximately 76.5% at the 0.75:1 [SH]:[ene] ratio. The addition of 0.25 and 0.4 equiv of Tz-NHS relative to the initial amount of norbornene groups increased the conversion to 89.5% and 94%, respectively. These results demonstrate that unreacted norbornenes are available for tetrazine-mediated functionalization, although a higher than expected amount of tetrazine was required to achieve near complete conversion.

3.3. Fluorescent Protein Conjugation with Tetrazine−Norbornene Click Reaction. To demonstrate the efficacy and selectivity of the tetrazine-norbornene click reaction, fluorescein-labeled ovalbumin was used as a model protein to visualize microparticle biotethering (Figure 5A−D). Microparticles were clearly seen fluorescing green under widefield fluorescence microscopy after incubation with tetrazine-functionalized fluorescein ovalbumin (Tz-Oval), indicating successful ovalbumin tethering. In contrast, minimal fluorescence was observed visually when the microparticles were incubated with fluorecein ovalbumin that was not tetrazine-functionalized (NF-Oval), indicating that unconjugated fluorophore was removed during PBS washing steps. The fluoresence of Tz-Oval, NF-Oval, and nonfunctionalized microparticles was also quantitatively analyzed on a flow cytometer (Figure 5E and Supporting Information, Figure S6). Surprisingly, the NF-Oval microparticles had measurable fluorescence by flow cytometry. Since ovalbumin, which has a hydrodynamic radius of approximately 3 nm, is small enough to diffuse through the polymer mesh, this result suggests that the fluorescent protein was not completely removed after washing. Nevertheless, there was a nearly 5-fold increase in the average fluoresence intensity for the particles treated with Tz-Oval.

3.4. Dose-Dependent ALP Bioactivity. To demonstrate conjugation of a bioactive protein we first chose ALP, which is a well-studied and characterized protein related to bone tissue

DOI: 10.1021/acs.biomac.6b00990
Biomacromolecules 2016, 17, 3516−3523

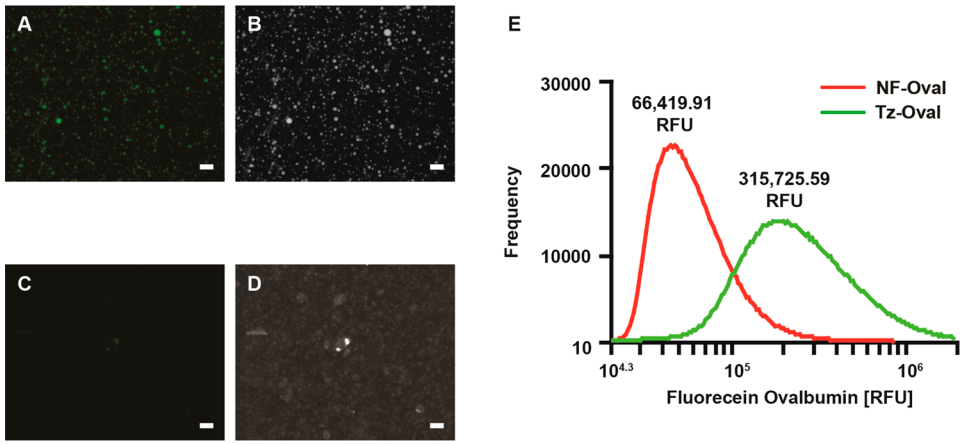

Figure 5. Selective conjugation of Tz-fluorescein ovalbumin to microparticles. (A,C) Fluorescence images of Tz-Oval microparticles and control NF-Oval microparticles, respectively, showing selective attachment of tetrazine functionalized protein. (B,D) Corresponding contrast-enhanced grayscale images for panels A and C, respectively, showing the presence of microparticles in the control image. Scale bars = 50 μm. (E) Frequency plot of relative fluorescence units (RFU) for both Tz-Oval and NF-Oval microparticles obtained by analysis on a flow cytometer, with average RFU values noted above each peak. A total of 900 000 particles were measured for each sample.

engineering.[46,47] As previously mentioned, one of the advantages for utilizing the bio-orthogonal tetrazine-norbornene click reaction is the lack of radical production during polymerization, which can affect protein bioactivity. After incubating microparticles with tetrazine-functionalized or nonfunctionalized ALP (Tz-ALP and NF-ALP, respectively, with NF-ALP being a negative control) bioactivity was confirmed based on pNPP substrate conversion to *p*-nitrophenol, which was monitored on a microplate reader (Figure 6). Importantly, the microparticles showed dose-dependent bioactivity after incubation with 0 mg/mL to 25 mg/mL of Tz-ALP, as shown by the plots of absorbance versus time. However, minimal bioactivity was observed for microparticles treated with NF-ALP as well as for microparticles that were treated with Tz-ALP but lacked norbornene groups (Figure S7). Quantitative analysis of the ALP activity based on the slopes of the absorbance-versus-time curves showed that the bioactivities of microparticles incubated with 6.25 mg/mL of Tz-ALP and higher concentrations were statistically higher ($p < 0.05$) compared to their negative control counterparts treated with equal NF-ALP concentrations (*). Bioactivity was also significantly increased with increasing Tz-ALP concentrations from 6.25 to 25 mg/mL (‡). These observations indicated increased ALP incorporation for Tz-ALP microparticles compared to NF-ALP microparticles, which was corroborated by protein loading measurements for the highest ALP concentration (Supporting Information, Figure S8).

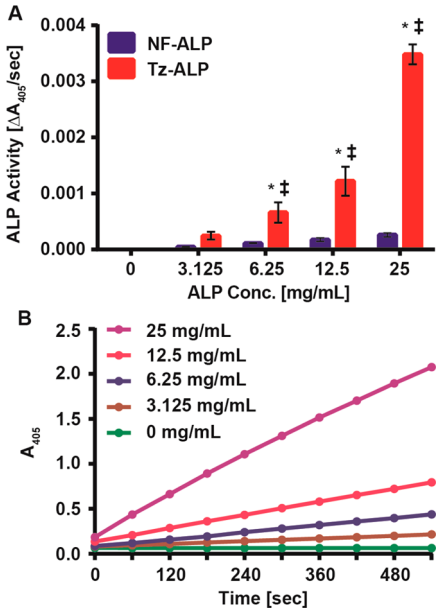

Figure 6. ALP bioactivity after microparticle functionalization. (A) Average ALP activity of Tz-ALP and NF-ALP microparticles with standard deviations. Data was analyzed by two-way ANOVA followed by post hoc comparisons (Tukey's method). The symbols * and ‡ indicate significant differences between Tz-ALP and NF-ALP and between Tz-ALP concentrations, respectively ($p < 0.05$). (B) Representative curves of absorbance versus time for microparticles functionalized with varying amounts of Tz-ALP and then incubated with the ALP substrate p-nitrophenyl phosphate.

In addition to measuring bioactivity via substrate consumption, mineralization is another important and measurable function of ALP bioactivity because of the enzyme's key role in mineralization *in vivo*.[48−51] Thus, mineralization was evaluated by incubating ALP-functionalized microparticles with calcium glycerophosphate and then staining with alizarin red S. Consistent with the ALP activity data collected using the p-nitrophenyl phosphate substrate, Tz-ALP-treated microparticles induced substantial mineralization, as indicated by robust red staining throughout the particles, whereas microparticles incubated with NF-ALP and calcium glycerophosphate control alone were not stained. Quantitative analysis by dye destaining and absorbance measurements confirmed that mineralization was significantly increased for the microparticles functionalized with Tz-ALP (Figure 7). Based on the staining results, the Tz-ALP microparticles appeared to act as nucleation sites for mineralization.

3.5. Dose-Dependent GOx Loading and Bioactivity.

To further demonstrate the versatility of our sequential click system, we chose GOx as a second bioactive protein. Importantly, GOx is widely used in glucose biosensing,[52−55] as it catalyzes the oxidation of D-glucose to gluconic acid and hydrogen peroxide in the presence of oxygen. This reaction can be quantitatively monitored *in vitro* using horseradish

DOI: 10.1021/acs.biomac.6b00990
Biomacromolecules 2016, 17, 3516−3523

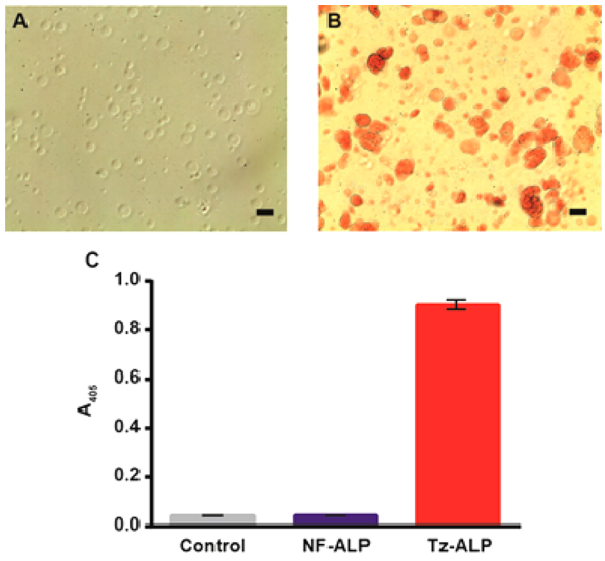

Figure 7. Quantifying ALP mineralization. (A) Bright field images of 25 mg/mL NF-ALP microparticles and (B) 25 mg/mL Tz-ALP microparticles after alizarin red S staining. Scale bars = 50 μm. (C) Average absorbance measurements at 405 nm after alizarin red S destaining with standard deviations. Statistical analysis confirmed a significant increase in mineralization for 25 mg/mL Tz-ALP group ($p < 0.05$).

peroxidase and an appropriate colorimetric substrate, such as *o*-dianisidine. Similar to ALP, the bioactivity of microparticles incubated with tetrazine-functionalized GOx (Tz-GOx) was quantified by monitoring the increase in absorbance due to D-glucose consumption/*o*-dianisidine oxidation over time (Figure 8). Similar to what was observed for microparticles functionalized with Tz-ALP, the absorbance-versus-time curves for microparticle bioactivity showed a concentration-dependent increase when functionalized with 0 mg/mL to 8 mg/mL of Tz-GOx. Analysis of the GOx activity, calculated from the slopes of the kinetic curves, showed that 2 mg/mL Tz-GOx and higher concentrations were statistically higher ($p < 0.05$) when compared to their negative control counterparts of equal NF-GOx concentration (*). The increases in enzyme activity as Tz-GOx concentration increased to 2, 4, and 8 mg/mL were also statistically significant (‡). These observations indicated increased GOx incorporation for Tz-GOx compared to NF-GOx, which was supported by protein loading measurements for the highest GOx concentration (Supporting Information, Figure S9).

4. CONCLUSION

This study demonstrates the novel use of sequential thiol−ene and tetrazine−norbornene click reactions to produce protein-functionalized bioactive hydrogel microparticles. The results show that facile control of microparticle size and maintenance of protein bioactivity/function after conjugation can be achieved. The polymerization and tethering mechanisms used here address the need for versatile, user-controlled chemical tools for synthesizing bioactive polymers. Additionally, because these click reactions are scalable and synthetically tractable for biomaterials, they are amenable to batch fabrication of bioactive materials. Taken together, this strategy of bioactive functionalization is a novel platform that can be employed for theoretically any protein of interest and shows promise for applications in tissue engineering, drug delivery, and biosensing.

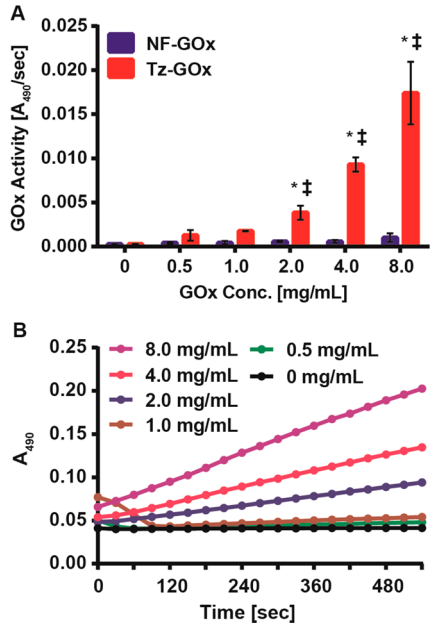

Figure 8. GOx bioactivity after microparticle functionalization. (A) Average GOx activity of Tz-GOx and NF-GOx microparticles with standard deviations. Data was analyzed by two-way ANOVA followed by post hoc comparisons (Tukey's method). The symbols * and ‡ indicate significant differences between Tz-GOx and NF-GOx and between Tz-GOx concentrations, respectively ($p < 0.05$). (B) Representative curves of absorbance versus time for microparticles functionalized with varying amounts of Tz-GOx and incubated with D-glucose, horseradish peroxidase, and *o*-dianisidine dye.

■ ASSOCIATED CONTENT

Supporting Information

The Supporting Information is available free of charge on the ACS Publications website at DOI: 10.1021/acs.biomac.6b00990.

NMR, additional experimental details, and data (PDF)

■ AUTHOR INFORMATION

Corresponding Author

*E-mail: dalge@tamu.edu.

Author Contributions

‖F.J. and R.Y. contributed equally to the synthesis of materials, collection of data, analysis of results, and preparation of the manuscript. D.L.A. provided inspiration and guidance for the project and manuscript preparation. H.P. performed GOx functionalization and bioactivity assays. J.K.C. contributed to microparticle analysis by flow cytometry. M.M. and A.K.G. contributed to microparticle characterization and manuscript preparation. All authors have read and given approval to the final version of the manuscript.

Funding

This research was funded through start-up funds to D.L.A. and A.K.G. from Texas A&M University and Texas A&M Engineering Experiment Station. M.M. acknowledges support from the NIH Director's Transformative Research Award (1R01EB016414).

Notes

The authors declare no competing financial interest.

DOI: 10.1021/acs.biomac.6b00990
Biomacromolecules 2016, 17, 3516−3523

■ ACKNOWLEDGMENTS

The authors thank Ms. Rachel Unruh for assistance with measuring GOx enzyme activity. R.Y. participated in this research through a visiting student program with SRM University. NMR and mass spectrometry characterization were performed in core facilities in the Department of Chemistry at Texas A&M University.

■ REFERENCES

(1) Kolb, H. C.; Finn, M. G.; Sharpless, K. B. *Angew. Chem., Int. Ed.* **2001**, *40* (11), 2004−2021.
(2) Hoyle, C. E.; Lowe, A. B.; Bowman, C. N. *Chem. Soc. Rev.* **2010**, *39* (4), 1355−1387.
(3) Kade, M. J.; Burke, D. J.; Hawker, C. J. *J. Polym. Sci., Part A: Polym. Chem.* **2010**, *48* (4), 743−750.
(4) Killops, K. L.; Campos, L. M.; Hawker, C. J. *J. Am. Chem. Soc.* **2008**, *130* (15), 5062−4.
(5) Lowe, A. B. *Polym. Chem.* **2010**, *1* (1), 17−36.
(6) Hoyle, C. E.; Bowman, C. N. *Angew. Chem., Int. Ed.* **2010**, *49* (9), 1540−73.
(7) Cramer, N. B.; Davies, T.; O'Brien, A. K.; Bowman, C. N. *Macromolecules* **2003**, *36* (12), 4631−4636.
(8) Fairbanks, B. D.; Schwartz, M. P.; Halevi, A. E.; Nuttelman, C. R.; Bowman, C. N.; Anseth, K. S. *Adv. Mater.* **2009**, *21* (48), 5005−10.
(9) McCall, J. D.; Anseth, K. S. *Biomacromolecules* **2012**, *13* (8), 2410−7.
(10) Lin, C.-C.; Raza, A.; Shih, H. *Biomaterials* **2011**, *32* (36), 9685−9695.
(11) Anderson, S. B.; Lin, C.-C.; Kuntzler, D. V.; Anseth, K. S. *Biomaterials* **2011**, *32* (14), 3564−3574.
(12) Gould, S. T.; Darling, N. J.; Anseth, K. S. *Acta Biomater.* **2012**, *8* (9), 3201−3209.
(13) Sawicki, L. A.; Kloxin, A. M. *Biomater. Sci.* **2014**, *2* (11), 1612−1626.
(14) Blackman, M. L.; Royzen, M.; Fox, J. M. *J. Am. Chem. Soc.* **2008**, *130* (41), 13518−13519.
(15) Saracoglu, N. *Tetrahedron* **2007**, *63* (20), 4199−4236.
(16) Hansell, C. F.; Espeel, P.; Stamenovic, M. M.; Barker, I. A.; Dove, A. P.; Du Prez, F. E.; O'Reilly, R. K. *J. Am. Chem. Soc.* **2011**, *133* (35), 13828−31.
(17) Devaraj, N. K.; Weissleder, R.; Hilderbrand, S. A. *Bioconjugate Chem.* **2008**, *19* (12), 2297−9.
(18) Devaraj, N. K.; Upadhyay, R.; Haun, J. B.; Hilderbrand, S. A.; Weissleder, R. *Angew. Chem., Int. Ed.* **2009**, *48* (38), 7013−7016.
(19) Carlson, J. C.; Meimetis, L. G.; Hilderbrand, S. A.; Weissleder, R. *Angew. Chem.* **2013**, *125* (27), 7055−7058.
(20) Han, H. S.; Devaraj, N. K.; Lee, J.; Hilderbrand, S. A.; Weissleder, R.; Bawendi, M. G. *J. Am. Chem. Soc.* **2010**, *132* (23), 7838−9.
(21) Alge, D. L.; Azagarsamy, M. A.; Donohue, D. F.; Anseth, K. S. *Biomacromolecules* **2013**, *14* (4), 949−953.
(22) Desai, R. M.; Koshy, S. T.; Hilderbrand, S. A.; Mooney, D. J.; Joshi, N. S. *Biomaterials* **2015**, *50*, 30−37.
(23) Alge, D. L.; Donohue, D. F.; Anseth, K. S. *Tetrahedron Lett.* **2013**, *54* (41), 5639−5641.
(24) van Hooy-Corstjens, C. S. J.; Saralidze, K.; Knetsch, M. L. W.; Emans, P. J.; de Haan, M. W.; Magusin, P. C. M. M.; Mezari, B.; Koole, L. H. *Biomacromolecules* **2008**, *9* (1), 84−90.
(25) Secret, E.; Kelly, S. J.; Crannell, K. E.; Andrew, J. S. *ACS Appl. Mater. Interfaces* **2014**, *6* (13), 10313−10321.
(26) Parlato, M.; Johnson, A.; Hudalla, G. A.; Murphy, W. L. *Acta Biomater.* **2013**, *9* (12), 9270−80.
(27) Utech, S.; Prodanovic, R.; Mao, A. S.; Ostafe, R.; Mooney, D. J.; Weitz, D. A. *Adv. Healthcare Mater.* **2015**, *4*, 1628.
(28) Griffin, D. R.; Weaver, W. M.; Scumpia, P. O.; Di Carlo, D.; Segura, T. *Nat. Mater.* **2015**, *14* (7), 737−44.
(29) Elbert, D. L. *Acta Biomater.* **2011**, *7* (1), 31−56.
(30) Liu, A. L.; García, A. J. *Ann. Biomed. Eng.* **2016**, *44* (6), 1946−1958.
(31) Young, C. J.; Poole-Warren, L. A.; Martens, P. J. *Biotechnol. Bioeng.* **2012**, *109* (6), 1561−70.
(32) Belair, D. G.; Khalil, A. S.; Miller, M. J.; Murphy, W. L. *Biomacromolecules* **2014**, *15* (6), 2038−48.
(33) Kawamoto, K.; Grindy, S. C.; Liu, J.; Holten-Andersen, N.; Johnson, J. A. *ACS Macro Lett.* **2015**, *4* (4), 458−461.
(34) Zhou, H.; Johnson, J. A. *Angew. Chem.* **2013**, *125* (8), 2291−2294.
(35) Cok, A. M.; Zhou, H.; Johnson, J. A. *Macromol. Symp.* **2013**, *329* (1), 108−112.
(36) Zhou, H.; Woo, J.; Cok, A. M.; Wang, M.; Olsen, B. D.; Johnson, J. A. Counting primary loops in polymer gels. *Proc. Natl. Acad. Sci. U. S. A.* **2012**, *109* (47), 19119−24.
(37) Zhou, H.; Schon, E. M.; Wang, M.; Glassman, M. J.; Liu, J.; Zhong, M.; Diaz Diaz, D.; Olsen, B. D.; Johnson, J. A. *J. Am. Chem. Soc.* **2014**, *136* (26), 9464−70.
(38) Fairbanks, B. D.; Schwartz, M. P.; Bowman, C. N.; Anseth, K. S. *Biomaterials* **2009**, *30* (35), 6702−6707.
(39) Shih, H.; Lin, C. C. *Biomacromolecules* **2012**, *13* (7), 2003−12.
(40) Bergmeyer, H. U.; Bergmeyer, J.; Grassl, M. *Methods of Enzymatic Analysis*, 3rd ed.; Verlag Chemie: Weinheim, Germany, 1983.
(41) Kawamoto, K.; Zhong, M.; Wang, R.; Olsen, B. D.; Johnson, J. A. *Macromolecules* **2015**, *48* (24), 8980−8988.
(42) Seliktar, D.; Zisch, A. H.; Lutolf, M. P.; Wrana, J. L.; Hubbell, J. A. *J. Biomed. Mater. Res.* **2004**, *68* (4), 704−16.
(43) Zisch, A. H.; Lutolf, M. P.; Ehrbar, M.; Raeber, G. P.; Rizzi, S. C.; Davies, N.; Schmokel, H.; Bezuidenhout, D.; Djonov, V.; Zilla, P.; Hubbell, J. A. *FASEB J.* **2003**, *17* (15), 2260−2.
(44) Tokatlian, T.; Shrum, C. T.; Kadoya, W. M.; Segura, T. *Biomaterials* **2010**, *31* (31), 8072−80.
(45) Van Hove, A. H.; Antonienko, E.; Burke, K.; Brown, E., 3rd; Benoit, D. S. *Adv. Healthcare Mater.* **2015**, *4* (13), 2002−11.
(46) Beertsen, W.; van den Bos, T. *J. Clin. Invest.* **1992**, *89* (6), 1974−80.
(47) Douglas, T. E.; Messersmith, P. B.; Chasan, S.; Mikos, A. G.; de Mulder, E. L.; Dickson, G.; Schaubroeck, D.; Balcaen, L.; Vanhaecke, F.; Dubruel, P.; Jansen, J. A.; Leeuwenburgh, S. C. *Macromol. Biosci.* **2012**, *12* (8), 1077−89.
(48) Robison, R. *Biochem. J.* **1923**, *17* (2), 286−93.
(49) Henrichsen, E. *Acta Orthop. Scand.* **1958**, *29* (34), 5−85.
(50) Hessle, L.; Johnson, K. A.; Anderson, H. C.; Narisawa, S.; Sali, A.; Goding, J. W.; Terkeltaub, R.; Millan, J. L. *Proc. Natl. Acad. Sci. U. S. A.* **2002**, *99* (14), 9445−9.
(51) Narisawa, S.; Yadav, M. C.; Millan, J. L. *J. Bone Miner. Res.* **2013**, *28* (7), 1587−98.
(52) Unruh, R. M.; Roberts, J. R.; Nichols, S. P.; Gamsey, S.; Wisniewski, N. A.; McShane, M. J. *J. Diabetes Sci. Technol.* **2015**, *9* (5), 985−92.
(53) Roberts, J. R.; Park, J.; Helton, K.; Wisniewski, N.; McShane, M. J. *J. Diabetes Sci. Technol.* **2012**, *6* (6), 1267−75.
(54) Brahim, S.; Narinesingh, D.; Guiseppi-Elie, A. *J. Mol. Catal. B: Enzym.* **2002**, *18* (1), 69−80.
(55) Guiseppi-Elie, A.; Brahim, S.; Slaughter, G.; Ward, K. R. *IEEE Sens. J.* **2005**, *5* (3), 345−355.

DOI: 10.1021/acs.biomac.6b00990
Biomacromolecules 2016, 17, 3516−3523